

Optimized ANN-fuzzy MPPT controller for a stand-alone PV system under fast-changing atmospheric conditions

Louki Hichem¹, Omeiri Amar¹, Merabet Leila²

¹Electrical Laboratory of Annaba, Faculty of Technology, Badji Mokhtar-Annaba University, Annaba, Algeria

²Electromechanical Systems Laboratory, Faculty of Technology, Badji Mokhtar-Annaba University, Annaba, Algeria

Article Info

Article history:

Received Oct 27, 2022

Revised Dec 29, 2022

Accepted Feb 5, 2023

Keywords:

Artificial neural network

DC-DC boost converter

Fuzzy logic technique

Hybrid method artificial neural network-fuzzy

Maximum power point tracking

Solar panel

ABSTRACT

Solar energy is one of the most promising renewable energy resources. Over the last few decades, photovoltaic (PV) systems have grown in popularity. Since the maximum power point (MPP) of a solar system changes with environmental circumstances, the maximum power point tracking (MPPT) technique is required to get the most power out of the solar system. Various MPPT techniques based on classical and artificial intelligence (AI) methodologies have been proposed in the literature so far. In this paper, we aim to provide a thorough comparative analysis of the most widely used MPPT algorithms based on AI. The MPPT techniques discussed are based on fuzzy logic (FL), artificial neural networks (ANN), and the suggested hybrid approach ANN-fuzzy. The designed MPPT controllers are evaluated in the same PV system, which consists of a PV module, a DC-DC boost converter, and a DC load, under the same weather profile. Using the MATLAB/Simulink simulation tool, the tracking accuracy, response time, overshoot, and steady-state ripple of each method are tested in different weather conditions. The simulation results show that the ANN-fuzzy proposed tactic outperforms both the FL and the ANN MPPT controllers in correctly and successfully tracking the maximum power under diverse atmospheric conditions.

This is an open access article under the [CC BY-SA](https://creativecommons.org/licenses/by-sa/4.0/) license.



Corresponding Author:

Louki Hichem

Electrical Laboratory of Annaba, Faculty of Technology, Badji Mokhtar-Annaba University

B.P 12, Annaba 23000, Algeria

Email: hichem.louki@univ-annaba.org

1. INTRODUCTION

The need for energy is increasing daily despite the depletion of fossil fuel resources. They create enormous environmental harm and are hazardous to our health, necessitating the development of new energy sources. Renewable energy sources, including wind, tides, hydroelectric, geothermal, and solar energy, might provide a workable solution to these problems. Solar energy is one of the most durable kinds of alternative energy since it is not only clean, but it is also inexhaustible, it does not cost anything, and it has a very long lifetime. The energy consumed on earth is around ten thousand times less than the energy supplied by the sun. As a result, it is vital to build instruments that will use unlimited energy sources via a photovoltaic (PV) system.

PV panels are instruments that use the photoelectric effect to turn sunlight directly into electricity. The fundamental component of the PV solar system is a group of solar cells [1]. The worldwide PV energy market grow significantly in 2021. At least 175 GW of PV systems were erected and commissioned last year. At the end of 2021, total cumulative PV installed capacity will reach at least 942 GW [2]. In 2022, the amount of solar power installed around the world is expected to go over 1.1 TW for the first time ever. This

is possible because the price of solar energy fell by an impressive 90% between 2009 and 2021. This made solar a worldwide phenomenon and led many countries to adopt this clean energy technology [3].

In light of this, Algeria has started a comprehensive effort to develop renewable energy sources in order to diversify its energy supply and encourage sustainable energy use. Algeria's energy strategy is primarily focused on the development of solar energy, which is motivated by the country's vast solar potential [4]. The initiative calls for the construction of a 1,000 MW PV solar power plant, which will be distributed around the country in lots ranging from 50 to 300 MW. It is part of a national renewable energy initiative with the goal of deploying 15,000 MW by 2035 [5].

The PV module's output characteristics, current-voltage (I-V) and power-voltage (P-V), are nonlinear and heavily influenced by climatic circumstances (irradiance and temperature) that affect the performance of a PV system. Consequently, variations in irradiance have an impact on PV output current, whereas changes in temperature have an influence on PV output voltage. However, PV systems are designed to operate at their maximum output power levels regardless of solar irradiation intensity or temperature. In order to improve the efficiency of a PV system, a DC-DC boost converter is required between the PV panel and the direct current (DC) load.

The maximum power point tracking (MPPT) control unit adjust the duty cycle of the DC-DC boost converter in real time and controls the switch (metal oxide semiconductor field-effect transistor (MOSFET) or insulated-gate bipolar transistor (IGBT) of the converter. As a result, the system produces its maximum amount of power regardless of the prevailing weather conditions. To optimize PV power, researchers developed numerous MPPT algorithms, like fractional open-circuit voltage [6], [7], short-circuit current [6], [8]. These methods are based on the linear relationship between the maximum power point (MPP) current or voltage and the corresponding values for the short-circuit current and open-circuit voltage. The most common method for determining maximum power is the perturb and observe (P&O) method [9]-[13], due to its ease of implementation. This technique works by periodically perturbing the terminal voltage of the PV module and then comparing the PV output power to the power output during the preceding cycle of perturbation. When the operating voltage of the PV module varies and its power rises, the control system adjusts the operating point accordingly. If the condition is not satisfied, the operating point is shifted in the other direction [10]. Incremental conductance (IC) [14]-[17] is a well-known method based on a mathematical model. This algorithm computes the derivative of the output power of the panel from the voltage (V) and its difference dV as well as the current I and its difference dI . Its derivative is zero at maximum power, whereas it is positive to the left and negative to the right [10]. These methods belong to the conventional approaches for monitoring the highest power point MPPT delivered by PV systems. The PV panel is removed from the system in order to measure the short-circuit current and open-circuit voltage in the first two methods. With the panel being isolated for short periods of time, energy is being wasted. On the other hand, IC and P&O are more common. These methods make use of a PV panel's (P-V) characteristics. After the MPP is determined, steady-state oscillations occur for P&O because of the perturbations made by this strategy to maintain the MPP, increasing the loss of power. The IC principle considers the slope of the P-V characteristic to be zero at MPP, and thus, theoretically, there is no more fluctuation once MPP is identified. As a result, fluctuations are dampened considerably. However, in practice, the zero value on the PV characteristic slope is rarely seen because of how digital processing works. As a result, the IC technique may generate an imprecise response when the irradiation is rapidly increased [12].

To deal with these problems, the MPPT control strategies were developed. They are mainly based on artificial intelligence (AI) techniques like fuzzy logic (FL), artificial neural networks (ANN), genetic algorithm (GA), neuro-fuzzy technique, and other techniques. They are more appropriate than conventional methods in order to enhance the response time, tracking efficiency, and minimization of overshoot in the transitional phase, as well as oscillation around the MPP under irradiation and/or temperature variations. Research by Algarín *et al.* [18], a P&O controller is described, and its performance is compared to that of a fuzzy controller able to detect the MPP of a PV array. The simulation findings indicate that the fuzzy controller is superior to the traditional controller in terms of convergence time, power waste, and oscillation around the operational point. A comparative analysis of four different MPPT algorithms that are based on FLC can be found in [19]. Asif *et al.* [20] recommended the conception and evaluation of an insulated PV system equipped with a push-pull converter and a MPPT algorithm based on FL. Research by Messalti *et al.* [21], both the fixed and variable step-size ANN-MPPT controllers were proposed, analyzed, and compared. Toure *et al.* [22] do research on a hybrid controller for solar system MPPT based on an ANN using MATLAB/Simulink. The researchers presented a new FL-based hybrid technique [23] to enhance MPPT. The algorithm presented by researchers consists of two parts. One of which includes operational point calculation and the other of which is accurate adjustment. Short circuit current is used to calculate the operation point, which predicts the estimated maximum power. Accurate adjustment is based on the FL approach and follows the accurate value of the power point. The proposed technique is simulated in MATLAB/Simulink. Kumar *et al.* [24] show the advantages of using the GA over P&O and IC. The authors

conclude, after studying a variety of methodologies in [25], that machine learning, FL, and AI techniques appear to be the most useful and promising in the process of harvesting the most power from a solar PV system. According to [26] and [27], different intelligent MPPT approaches are grouped into three categories: offline, online, and hybrid methods. Each category's simulation results were also compared using MATLAB/Simulink. Soft computing methods based on MPPT have recently been reviewed in [28]. A thorough categorization of MPPT approaches has been published in [29]. A full overview of the principles of MPPT approaches is provided, as well as a comparison of certain critical parameters. Many reviews have established the feasibility of using AI approaches in PV system MPP trackers for modeling, prediction, and control. These have lately been developed and are utilized to increase the effectiveness of energy conversion. On the other hand, rapid advancements in field programmable gate arrays (FPGAs) offer excellent chances to integrate MPPT trackers based on AI approaches effectively for real-time applications. More research is being conducted to take advantage of potential trends and challenges in the design of MPPT trackers incorporating intelligent digital controllers in an FPGA, as mentioned in [30]. During research, special factors such as cost, complexity of implementation, efficiency, convergence speed, overshoot, and possible practical implementation are evaluated. Based on the combination of ANN and the FL approach, an optimal and effective hybrid solution for tracking a PV panel's maximum power point (MPPT) is presented in this work. This hybrid approach will be evaluated against both approaches. ANN and FL are each used separately in various environmental conditions (irradiation and temperature). Based on simulations conducted with MATLAB/Simulink, key metrics for each approach, including efficiency, time response, overshoot, and oscillation in the steady state regime, were compared.

The paper is structured as follows: after the introduction in section 1, a description of the PV system is presented in the following section. Section 2 describe pv system, section 3 describes the three MPPT strategies and includes details on the FL MPPT model, ANN, and proposed hybrid tactic ANN-fuzzy employed in this study. In section 4, the simulation results are analyzed and compared. For conclusion describes in section 5.

2. PHOTOVOLTAIC SYSTEM

As part of this research, a standalone PV system is taken into account. A PV panel, a DC-DC boost step-up converter, a MPPT controller, and a resistive DC load make up the components of the system, as shown in Figure 1. The system contains different parts, which will be developed in the following paragraphs.

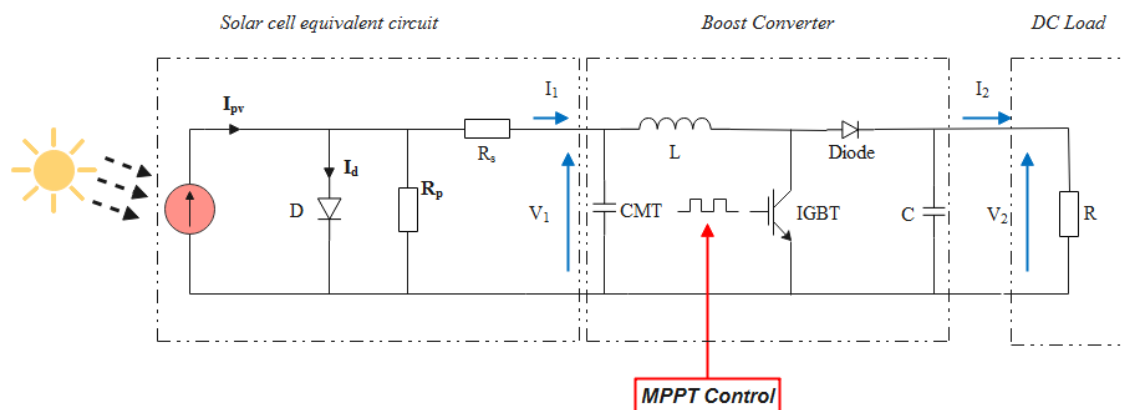


Figure 1. PV system

2.1. Solar panel

A variety of models are employed to reflect the properties of the PV source. The single-diode model is the most widely used model, which is noted for its precision, simplicity, and moderate computing effort. The goal of this model is to characterize the PV source under various radiation and temperature circumstances. As a result, the (I-V) characteristic is described as (1):

$$I_{pv} = I_{ph} - I_o \left[\exp \left(\frac{V_{pv} + I_{pv} R_s}{n N_s V_t} \right) - 1 \right] - \frac{V_{pv} + I_{pv} R_s}{R_{sh}} \quad (1)$$

Where I_{ph} signifies PV current, I_o denotes diode saturation current, n denotes diode ideality factor, R_s is the series resistance of the PV module, R_{sh} is the parallel resistance of the PV panel, N_s is the number of cells in one

module, and I_{pv} is the output current. The output voltage is V_{pv} , and the thermal voltage is V_t [6]. Figures 2 and 3 depict the I-V and P-V characteristics for different light intensities and temperatures. As indicated in Figure 3, open circuit voltage has an inverse relationship with temperature, which means that as the temperature rises, open circuit voltage and maximum power drop, whereas short circuit current and light intensity have a direct relationship. Short circuit current and maximum power rise as light intensity increases [23].

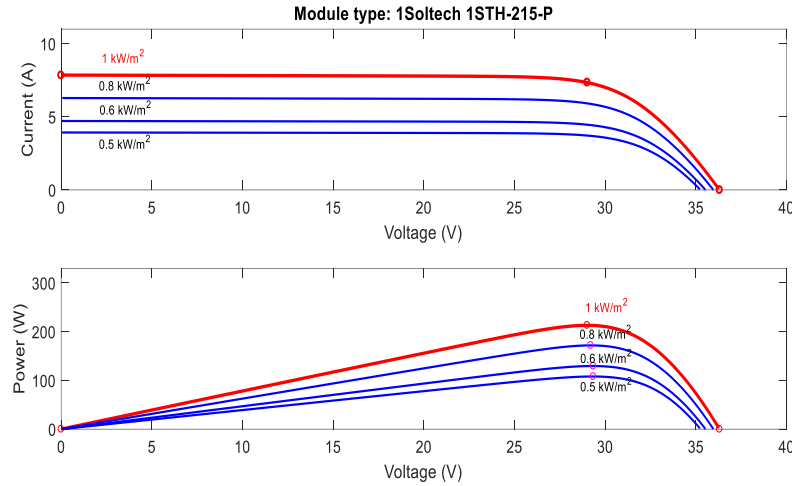


Figure 2. I-V and P-V characteristics under different irradiation levels

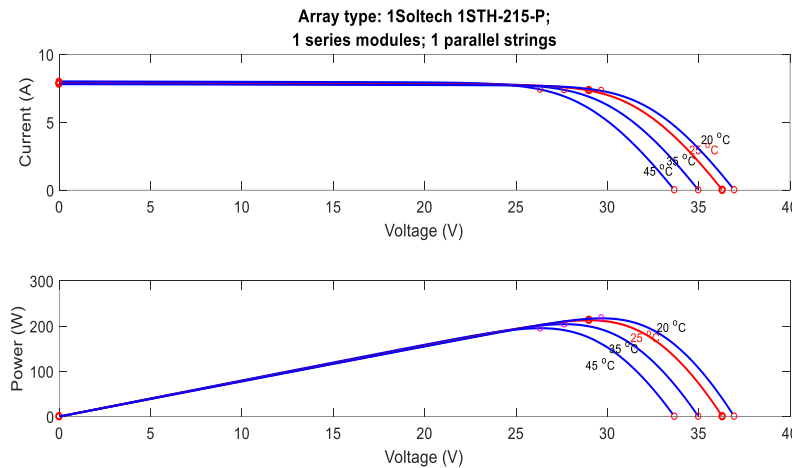


Figure 3. I-V and P-V characteristics under different temperature levels

2.2. Modeling of boost converters

A DC-DC step-up converter is positioned in this configuration between the PV panel and the load in order to extract the maximum amount of power possible from the panel. It is employed for the purpose of matching the load to the solar panel [23]. Figure 4 shows the boost DC-DC converter circuit. The DC voltage at the input of the DC-DC converter is provided by the PV solar panel. The converter duty cycle D is the most important and crucial factor in selecting the boost converter components and IGBT control in order to optimize the harvested power from the solar PV system [31]. The relationships between input and output voltages and currents of the boost converter can be written as (2):

$$V_{out} = V_{in} \frac{1}{1-D} \quad (2)$$

$$I_{out} = I_{in}(1-D) \quad (3)$$

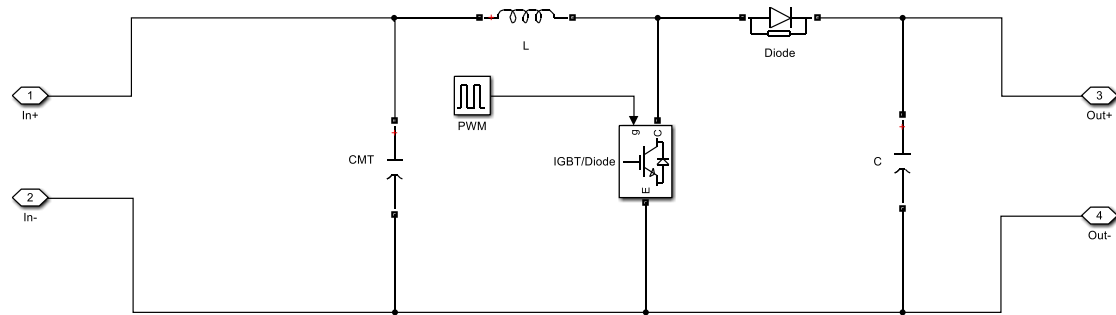


Figure 4. Boost converter

3. MPPT TECHNIQUES

Because the maximum available power of solar arrays varies with the weather, a real-time MPPT is an essential element of the PV system. The goal of an MPPT controller is to be able to monitor the MPP under various climatic conditions (irradiance and temperature). This control has been designed with the intention of making an automated adjustment to the duty cycle so that it is brought to the MPP. Numerous MPPT techniques have been developed in scientific research to solve these problems. Accuracy, tracking effectiveness, response time, overshoot in the transient phase, oscillation around the MPP at steady state, and cost are the parameters that will be utilized to evaluate the various MPPT approaches presented by the researchers [21].

3.1. Fuzzy logic technique

One of the most successful MPPT optimization strategies is FL. Numerous studies, including [31]-[42], have used FL to make the PV work around the MPP [36]. As shown above, climate is the primary effect on the non-linear features of the I-V and P-V characteristics. FL control has several benefits. It doesn't need exact mathematical modeling and can manage non-linearity and imprecise inputs. However, background information is required for FL controller design [4]. In order to keep tabs on the MPP that PV systems generate, FL was utilized, as mentioned in section 1. It is used to improve the efficiency of traditional MPPT techniques (such as P&O, IC, or proportional integral derivative (PID)) or in tandem with other AI-based methods like ANNs or GAs. Hill climbing method (HC), P&O, and IC are examples of traditional MPPT approaches based on fixed step-size that have significant drawbacks, including slow convergence, oscillations around the MPP, and an inability to follow the MPP during abrupt changes in atmospheric conditions (irradiation and temperature). Larger step sizes allow for faster follow-up, but excessive steady-state oscillations are inevitable. On the other hand, oscillations can be minimized by using a smaller step size with slower dynamics. The step size should provide an acceptable trade-off between dynamics and oscillations depending on the operational environment (irradiation, temperature) [21]. The FL controller FLC will offer a variable step size to get over these issues. The step size will be set by the membership functions and inference rules, which have improved system performance in both permanent and temporary regimes by adapting to weather circumstances. The FLC's primary steps can be divided into three categories: fuzzification, inference rules, and defuzzification. A FL controller composed of two inputs, one output, and 25 rules shown in Table 1 [36] is proposed. The synoptic scheme of the PV system using the FL MPPT technique is shown in Figure 5. E and CE are the fuzzy controller variable inputs defined using (4) and (5):

$$E(k) = V(k) - V_{mpp} \quad (4)$$

$$CE(k) = E(k - 1) - E(k) \quad (5)$$

Where V_{mpp} is the MPP, $V(k)$ is the instantaneous voltage of the solar panel observed at sample time k , $E(k)$ represents the error between $V(k)$ and V_{mpp} at the sample time k , and $CE(k)$ represents the error change at sampling time k . Duty cycle D is the output variable. The variables are transmitted to the deduction unit after being fuzzified, and after applying the rules, they move into the defuzzification stage. Then, a real value of the duty cycle D is then generated by the controller [23]. The membership functions for the input variables E and CE are depicted in Figures 6 and 7, respectively, while the membership function for the output duty cycle D is represented in Figure 8.

Table 1. The 25 rules of the FL controller

ECE	NB	NS	Z	PS	PB
NB	Z	Z	Z	B	M
NS	Z	Z	S	M	B
Z	Z	S	M	B	VB
PS	S	M	B	VB	VB
PB	M	B	VB	VB	VB

*NB is negative big; NS is negative small; Z is zero; PS is positive small; PB is positive big; S is small; M is medium; B is big; VB is very big

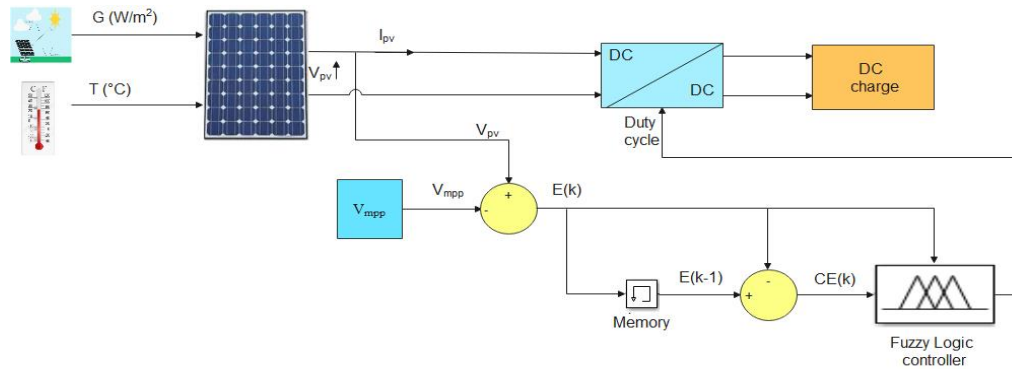


Figure 5. Synoptic schematic of a solar system using FL MPPT

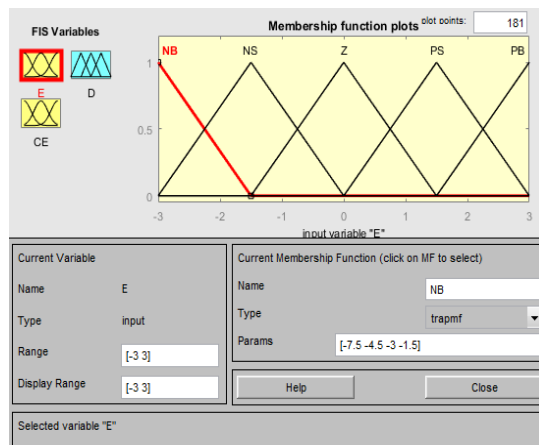


Figure 6. Membership function of error for FL MPPT

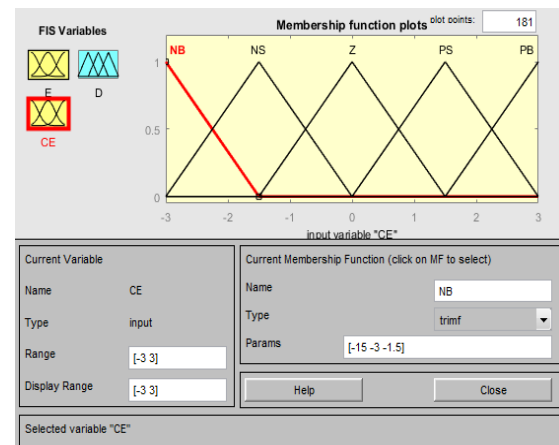


Figure 7. Membership function of change of error for FL MPPT

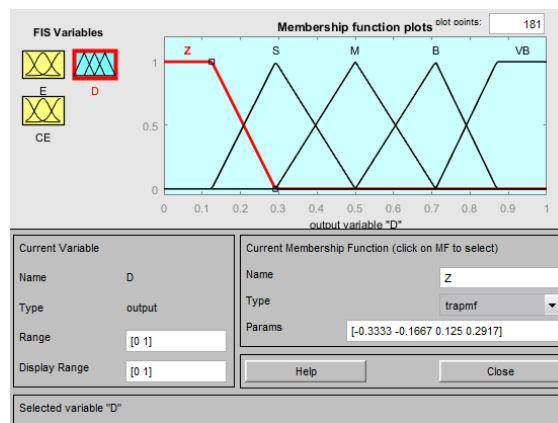


Figure 8. Membership function of duty cycle for FL MPPT

3.2. Artificial neural networks MPPT algorithm

ANN approaches have been regarded as one of the greatest alternatives for computational systems over the last few decades due to the numerous advantages they offer over traditional computational systems. They are able to deal with some complicated and non-linear problems without the need for an exact mathematical model. An ANN is a data-processing system made up of numerous artificial neurons, which are conceptually comparable to biological brain cells in that they are simple, densely linked processors. These neurons are linked together by many weighted linkages that allow for the transmission of electric signals. Each neuron has several connections that send information in but only one that transmits data out. When it comes to learning and recognizing patterns, these neural networks really shine. As shown by recent applications, there is great hope for the use of ANNs in solving complex data processing and interpretation problems. ANN are seen as a good fit for applications involving PV systems, notably in the monitoring of the MPP for a PV system [22], due to their efficacy in system identification and adaptive controls. To reach MPP, we use a pair of ANN to monitor the peak power point (see Figure 9).

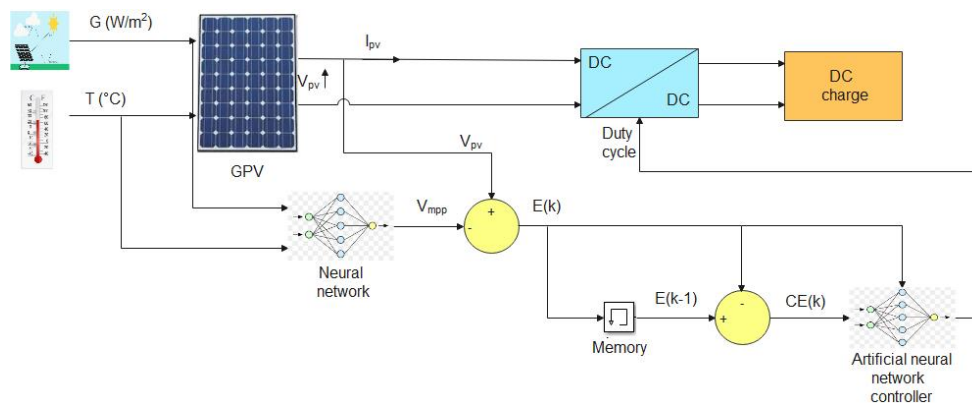


Figure 9. Synoptic schematic of a solar system using the ANN MPPT method

The first network is a multi-layer feed-forward neuron system that accounts for irradiance and temperature changes (see Figure 10). There are three distinct parts to the multilayer neural network's architecture. Two neurons make up the input layer, and the data they receive are the sun's intensity and the ambient temperature. The number of neurons in the hidden layer, ten, was arrived at by utilizing the empirical rule, which suggests that one should begin with a high number of neurons and progressively lower them until one has a more stable network with more precise outputs. The output layer is made up of just one neuron, whose MPP is where its optimal voltage is (see Figure 10).

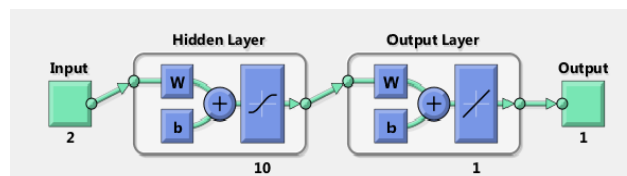


Figure 10. Feed-forward neural network

It should be noted that numerous attempts to enhance the accuracy of the ANN developed led to the adoption of this structure. Through a brief MATLAB code generation, the data used to train the ANN controller is acquired in order to complete the learning process. The dataset contains both the input values (irradiance and temperature) and the output target MPP voltage (V_{mpp}). All the data needed for training in offline mode can be found in the MATLAB workspace after executing the program MATLAB [43]. To increase prediction accuracy, datasets used to train neural networks must contain a large set of measurements [4]. It can be trained in a variety of ways. The Levenberg-Marquardt approach [44] is utilized to train the ANN in this research (see Figure 11). It was observed that the Levenberg-Marquardt (LM) algorithm is the optimum training function for tracking the MPPT from PV panels regardless of the weather (irradiation and temperature).

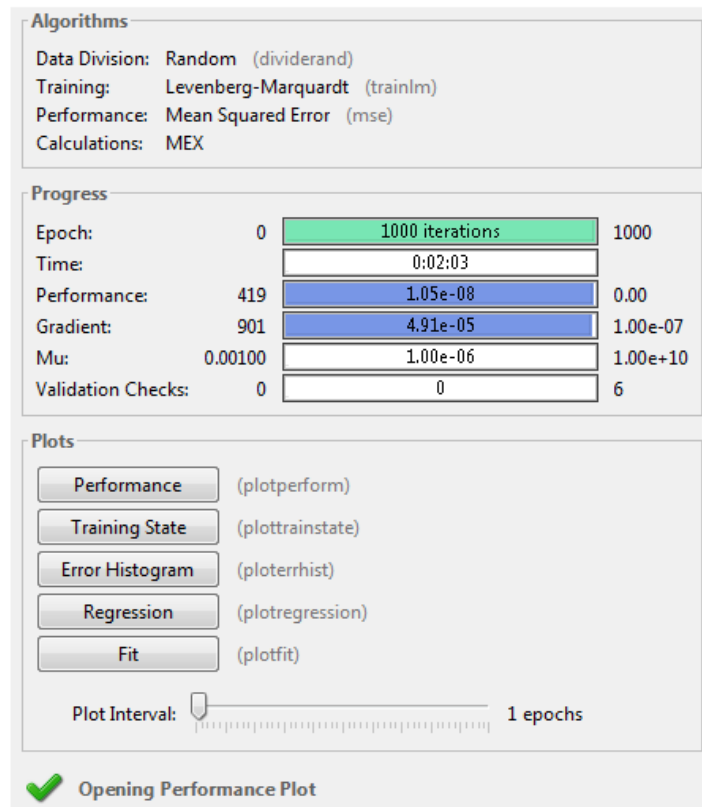


Figure 11. Training ANN

The performance was evaluated using the mean square error (see Figure 12). Faster convergence, a smaller mean square error, as well as a greater regression coefficient were all attained via feed-forward networks (see Figure 13). This paper's presented ANN-based MPPT approach can follow MPP under a variety of environmental circumstances (sun irradiance and temperature) [45].

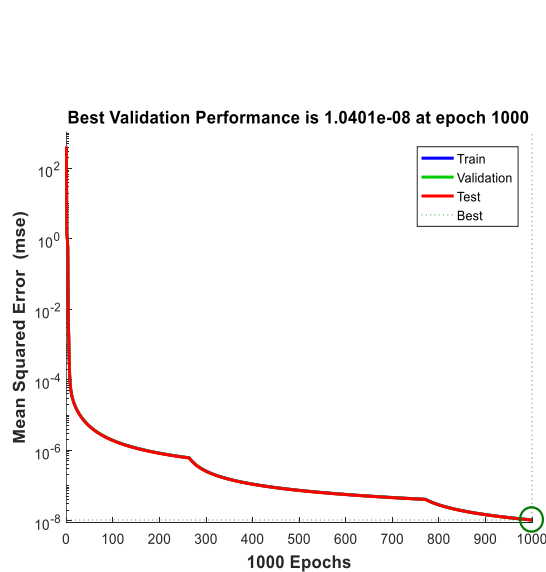


Figure 12. Mean square error vs epochs

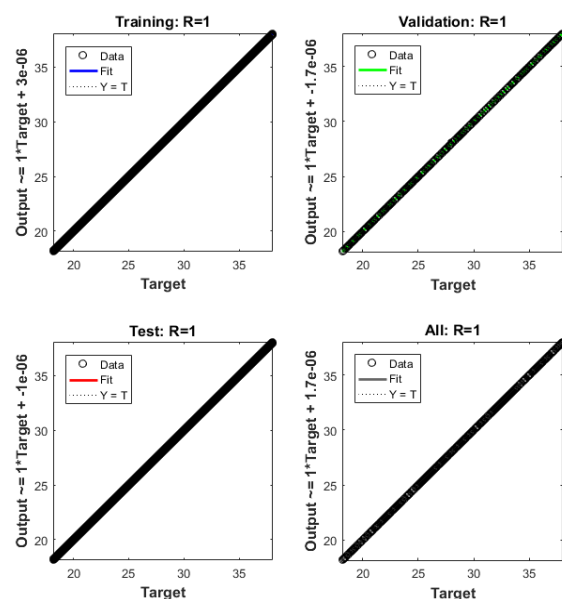


Figure 13. Regression coefficient

To cover the majority of situations in the most geographical locations of the world, the temperature (T) ranges from $0\text{ }^{\circ}\text{C}$ to $55\text{ }^{\circ}\text{C}$ with random variation (the variation step changes randomly) and the solar irradiation (G) ranges from 100 W/m^2 to $1,000\text{ W/m}^2$ to cover most cases of insolation (low, medium, and high levels of irradiation). This dataset was used to train the first neural networks (offline mode). It was divided into 70% for learning, 15% for testing, and 15% for validation data. After each training, the learned ANN models are continuously updated to build stable and precise neural networks, and the outcomes are tested and maintained. When it comes to convergence, a performance factor that determines how well the networks operate. To keep track of how well models are performing, validation data is employed. If the networks perform as well on both the test and validation data, we may conclude that they are accurate in generating the optimal voltage when activated by these inputs (G, T) [22]. After training the ANN and specifying the neuron weights, the output is now automatically related to V_{mpp} in the case of any T and G as ANN inputs [44].

The structure, activation function, and training procedure of the second neural network are identical to those of the first. A large amount of data is employed to train the second neural network in offline mode in order to enhance the prediction accuracy. The error E and the variation of the error CE , which are described by (4) and (5), are the respective inputs of the second neural network, whereas the output of the second neural network is the duty cycle. The standalone PV system is simulated using MATLAB/Simulink and consists of a PV module coupled to a DC-DC boost converter whose IGBT switch is controlled by a unit of control that is based on a trained ANN model.

3.3. ANN-fuzzy MPPT

FL and ANNs are combined in the ANN-fuzzy method. It is an improved effective hybrid method which is proposed for monitoring the MPP of a PV panel. The ANN (Figure 14) used to calculate the optimal voltage V_{mpp} based on environmental factors (such as sun irradiation and temperature) is structurally similar to the first ANN described in the previous section. In other words, the important aim of the ANN controller is to compute the V_{mpp} for every given combination of irradiance and temperature.

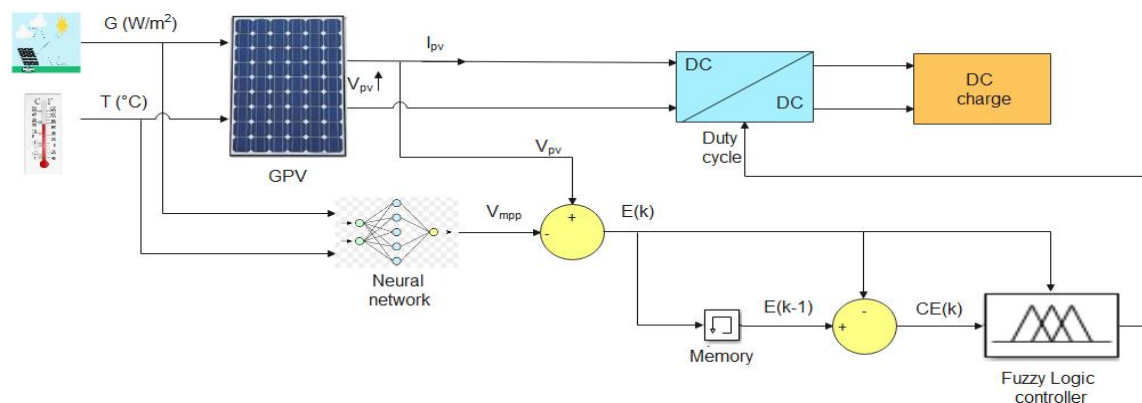


Figure 14. Synoptic schematic of a solar system using the ANN-fuzzy MPPT strategy suggested

Then, V_{mpp} is considered a reference value (target) that the PV module output voltage should follow in order to reach the optimum power point in various weather circumstances. To accomplish this task, the FL regulator gets involved. The goal is to reduce and remove the difference between the output voltage measured from the PV module at sampling time k and V_{mpp} by generating the appropriate duty cycle. A PWM generator drive the IGBT switch of the DC-DC boost converter in order to follow the highest power point of the PV module whatever the climatic conditions (irradiation and ambient temperature). The FL controller receives two inputs: the error $E(k)$ (Figure 15) and the change in the error $CE(k)$ (Figure 16), with the duty cycle D serving as the ultimate output of our proposed approach, which is displayed in Figure 17. In (4) and (5) of the preceding section are used to determine the error $E(k)$ and the variation in error $CE(k)$.

One of the most accurate ways to monitor the MPP is by using FL. It offers excellent technological features such as fast speed, precision, and efficiency. The cost of the controller rises as the number of rules grows, but it also becomes more precise while lowering speed, and adding more rules will increase complexity and expense. A system with high precision, few rules, and low cost is the perfect fuzzy system.

Therefore, by reducing the number of rules, we can minimize the cost of the FL controller while also making this technology easier to implement [33].

The suggested technique's most important advantage is the minimization of the number of FL controller rules to seven (see Table 2), as opposed to the 25 rules presented in [18], [32], [34], [38]. While there are some references such as in [41], use 36 rules and use 49 rules as mentioned in [20], [31], [40]. The aim of optimizing the number of rules in our proposed approach is to lower the expense of the MPPT technique while also making the technique simple to implement in real time. The presented hybrid technique includes seven rules, as shown in Table 2. It will also reduce the number of commutations that occur in converters, as a result, extending their lifespan. 15 KHz was used in the ANN-fuzzy proposed method instead of 20 kHz or more in the other publications in the literature such as [18], [32], [34], whose switching frequency is 20 kHz. In the case of [31], the switching frequency is 30 kHz. The following figures represent the membership functions of the two inputs $E(k)$ and $CE(k)$, as well as the output D (duty cycle).

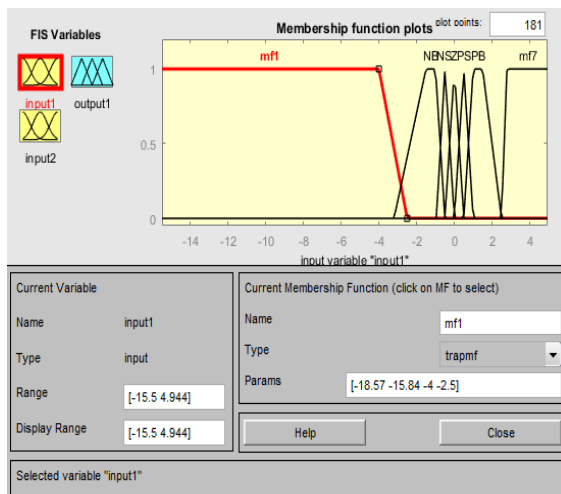


Figure 15. Membership function of error for ANN-fuzzy MPPT

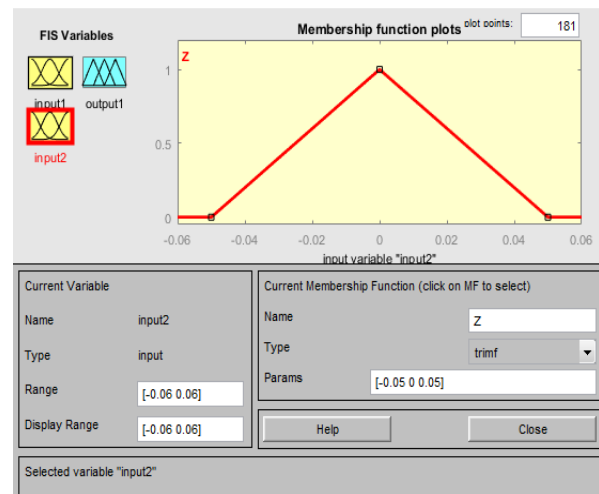


Figure 16. Membership function of change of error for ANN-fuzzy MPPT

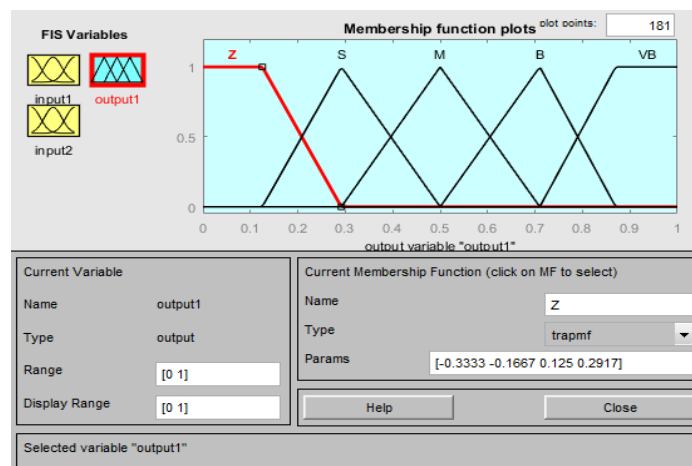


Figure 17. Membership function of duty cycle for ANN-fuzzy MPPT

Table 2. ANN-fuzzy MPPT controller rules

ECE	Mf1	NB	NS	Z	PS	PB	Mf7
Z	Z	Z	S	M	B	VB	VB

*Mf1: membership function number 1

*Mf7: membership function number 7

4. RESULTS AND DISCUSSION

To simulate the MPP tracking of the PV system based on the proposed MPPT controllers under varied weather circumstances (irradiation and temperature), the simulation program MATLAB/Simulink is employed. It is an adequate way to analyze the performance of each technique proposed above. The entire PV system is simulated and subjected to weather profiles, enabling testing in a range of situations to choose the best designed controller from the methodologies described in the earlier portions. The PV system depicted in Figure 1 includes a solar PV panel, which is a Soltech 1STH-215-P PV module (Table 3), and a DC-DC boost converter, which has a switching frequency of 15 kHz. The boost converter contains an input capacitor (300 μ F), an input inductance (45 μ H), and an output capacitor (300 μ F). A resistive load of 20 ohms serves as the output load. The MPPT approaches mentioned above are used to control the boost converter. The characteristics of the Soltech 1STH-215-P module are listed in Table 3.

4.1. Results under variations of irradiation

Figure 18 displays the irradiation profile, with an irradiation of 1,000 W/m^2 initially delivered from zero to 0.5 seconds. During the simulation, the temperature is kept at $T=25^\circ\text{C}$ in this instance, while abrupt changes in irradiation levels occur at 0.5 s, 1 s, and 1.5 s. Irradiation variations range from 1,000 W/m^2 to 500 W/m^2 , 500 W/m^2 to 800 W/m^2 , and lastly, 800 W/m^2 to 600 W/m^2 , as well as in Figure 19, which depicts the reactions of several MPPT control approaches under varied irradiation circumstances.

Table 3. Parameters of the PV module

Parametres	Values
Maximum power (P_{mpp})	213.15 W
Voltage at MPP (V_{mpp})	29 V
Current at MPP (I_{mpp})	7.35 A
Open circuit voltage (V_{oc})	36.3 V
Short circuit current (I_{sc})	7.84 A
Temperature coefficient of (V_{oc})	-0.36099%/°C
Temperature coefficient of (I_{sc})	0.102%/°C

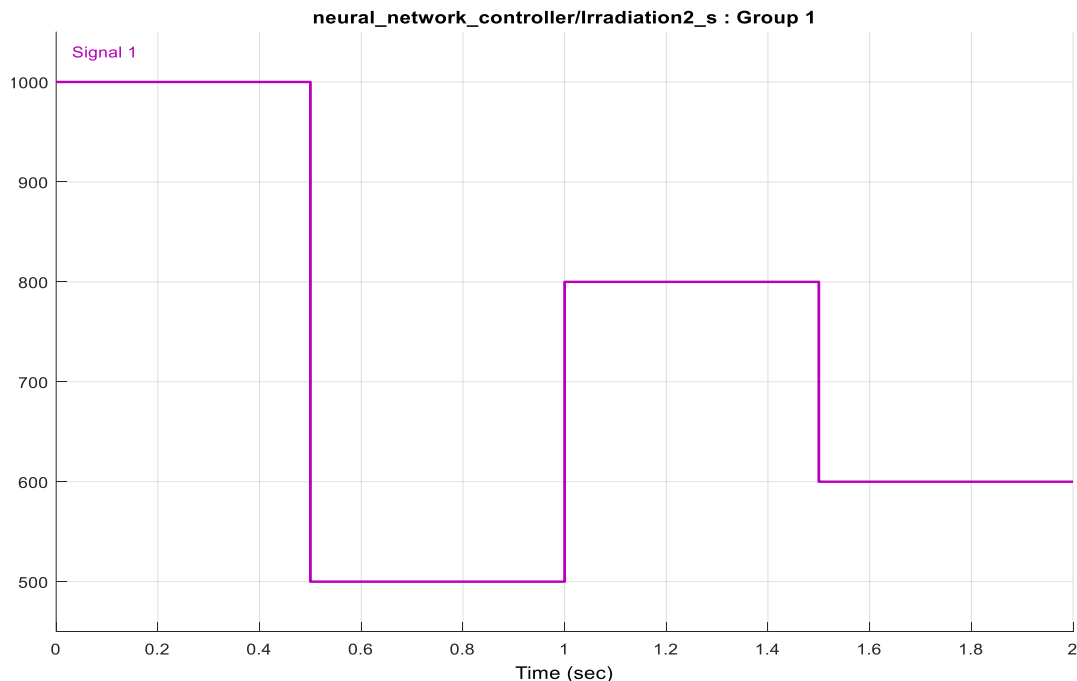


Figure 18. Simulation-used level of irradiation

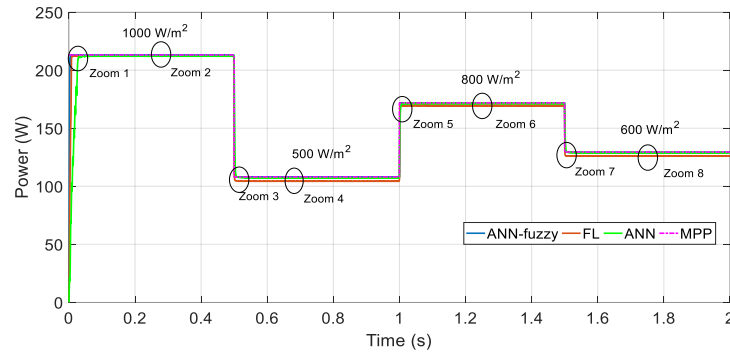


Figure 19. The output power of the PV system under scenario I of irradiation variation as simulated using the FL, ANN, and the proposed ANN-fuzzy MPPT techniques

Figures 20 and 21 depict MPP monitoring by the designed MPPT controllers, which are following the weather profile displayed above. For the initial interval $t \in [0, 0.5]$ s at STC conditions (standard test conditions: sun radiation $G=1000 \text{ W/m}^2$ and ambient temperature $T=25^\circ\text{C}$), all controllers tracked the MPP with sufficient precision. This is evident by the power levels being quite close to the theoretical value associated with the rate of irradiation and temperature in this circumstance. However, the ANN-fuzzy methodology obviously outperforms both the other methods in terms of tracking accuracy. This is demonstrated by the power value delivered by this unit of control, which is closer to the MPP than the values produced by both the FL and ANN MPPT controllers. According to Figure 20, the proposed ANN-fuzzy MPPT controller reacts to changes in irradiance and reaches the stationary operating point in less than 5 ms at start-up and for the STC conditions. The FL MPPT controller responds to changing irradiance in 10.94 ms, whereas the ANN MPPT controller takes 40 ms. So, the FL MPPT controller response time is 2,189 times slower than the ANN-fuzzy MPPT controller, while the ANN-fuzzy MPPT controller has a convergence speed that is eight times as fast as the ANN MPPT controller. From Figure 21, the suggested ANN-fuzzy algorithms perform well in steady state in STC weather conditions with a low steady-state oscillation of 0.1 W. This value corresponds to 0.047% of the power obtained with this method. In comparison to the ripple created by the FL technique, which is equal to 0.2 W (0.094%), the ANN algorithm caused a significant oscillation around the MPP of 0.4 W (0.18%). This resulted in a significant waste of energy for a PV system.

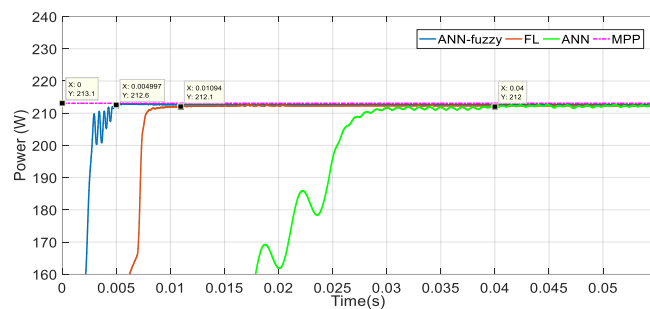


Figure 20. Response time of the FL, ANN, and ANN-fuzzy MPPT at start-up

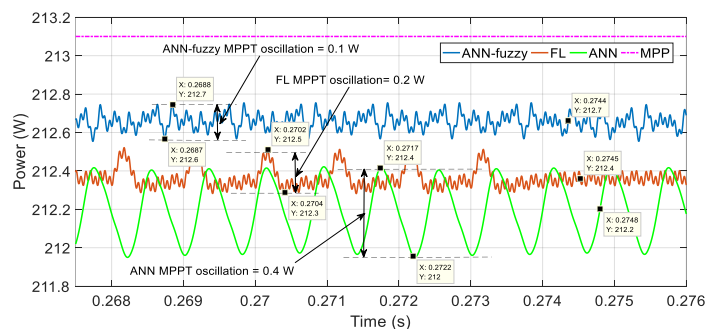


Figure 21. FL, ANN, and ANN-fuzzy MPPT power ripple techniques at start-up

Figures 22 and 23 illustrate MPP tracking using MPPT controllers developed and tested in compliance with the abovementioned weather profile. The irradiation drops from $1,000 \text{ W/m}^2$ to 500 W/m^2 for the second period $t \in [0.5, 1] \text{ s}$ while the temperature remains unchanged at $T=25^\circ\text{C}$. Both ANN-fuzzy and ANN controllers successfully tracked the MPP, and in both situations, the power values were extremely close to the predicted value related to the rate of irradiation and temperature in this case. Regarding the power value of the FL controller, it is less precise than the values of the ANN-fuzzy and ANN controllers. Moreover, in terms of tracking accuracy, the ANN-fuzzy methodology clearly exceeds both other approaches. Figure 22 shows that the suggested ANN-fuzzy MPPT controller responds to variations in irradiance and reaches the steady state operating point in 2 ms when the irradiance declines from 1000 W/m^2 to 500 W/m^2 at $T=25^\circ\text{C}$. When the sun's irradiance varies, the FL-MPPT controller reacts in 9.9 ms, whereas the ANN-MPPT controller takes 21.3 ms.

In addition to producing a less accurate power value than the other methods, the FL MPPT controller has a response time that is 4.95 times that of the ANN-fuzzy MPPT controller, whereas the ANN MPPT controller has a response time that is 10.65 times that of the ANN-fuzzy MPPT controller. The positive point for all approaches is that they do not produce any overshoot during the transient phase, which allows them to prevent energy loss during the transient regime. As shown in Figure 23, the proposed ANN-fuzzy algorithms and the ANN technique work well in steady state under meteorological conditions (sun irradiation $G=500 \text{ W/m}^2$ and temperature $T=25^\circ\text{C}$), with a low oscillation in steady state of 0.2 W for the ANN-fuzzy method. This value represents 0.185% of the power value achieved by this technique, and 0.2 W for the ANN method, which represents 0.186% of the power value reached by this technique. The power value provided by the FL algorithm is less accurate than the other two methods, with a steady state ripple of 0.2 W (0.191%).

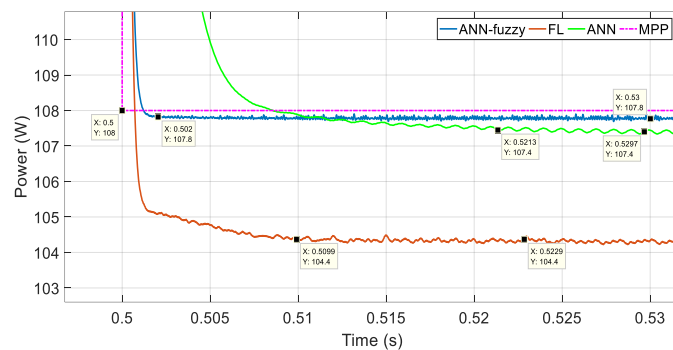


Figure 22. Response time of the FL, ANN, and ANN-fuzzy MPPT techniques during the change of insolation from $1,000 \text{ W/m}^2$ to 500 W/m^2

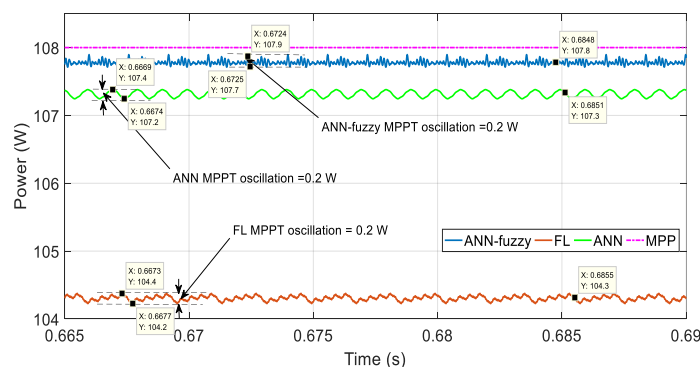


Figure 23. FL, ANN, and ANN-fuzzy MPPT power ripple during the change of insolation from $1,000 \text{ W/m}^2$ to 500 W/m^2

In accordance with the weather conditions described above, Figures 24 and 25 show the MPP tracking performed by the MPP monitoring systems outlined in the previous sections. The irradiation is

raised to 800 W/m^2 for the third period, $t \in [1, 1.5] \text{ s}$, while the temperature is maintained at $T = 25^\circ \text{C}$. The MPP has been closely monitored by the ANN-fuzzy and ANN controllers. In both situations, the power levels generated by these controllers are quite near to the expected values corresponding to the given irradiance and temperature level, especially for the ANN-fuzzy technique, which matches the theoretical value of the MPP correctly and with excellent precision. Although the power value of the FL controller is higher, it is less precise than the values of the ANN-fuzzy and ANN controllers, but it is acceptable in this case. In terms of tracking accuracy, the ANN-fuzzy methodology clearly outperforms both other approaches. As seen in Figure 24, when the solar irradiance is raised from 500 W/m^2 to 800 W/m^2 at $T = 25^\circ \text{C}$, the proposed ANN-fuzzy MPPT controller responds to changes in irradiance and reaches the steady-state operating point in 2 ms. When the irradiance increases, the FL controller reaches the steady state after 8 ms, while the ANN MPPT controller needs 12 ms.

Compared to other methods, the FL-MPPT controller provides an inaccurate power value, which in this case is relatively far from the expected theoretical power value for the specific irradiance and temperature. All techniques have the advantage of not overshooting during the transient phase, allowing them to prevent energy loss during the transient regime. According to Figure 25, the proposed ANN-fuzzy algorithm operates well in a steady state under the specified weather conditions, with a low steady state oscillation of 0.1 W for the ANN-fuzzy method, representing 0.058% of the power value reached by this technique. Regarding the ANN method, the oscillation around the MPP generated by this method in steady state is 0.4 W, which corresponds to 0.23% of the power value achieved by this technique, resulting in significant energy waste for a PV system. The FL algorithm provides a less precise power value than the other two approaches, with a ripple of 0.1 W (0.059%) at steady state.

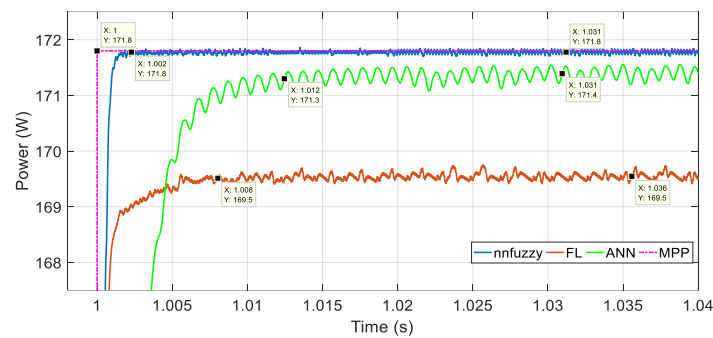


Figure 24. Response time of the FL, ANN, and ANN-fuzzy during the change of insolation from 500 W/m^2 to 800 W/m^2

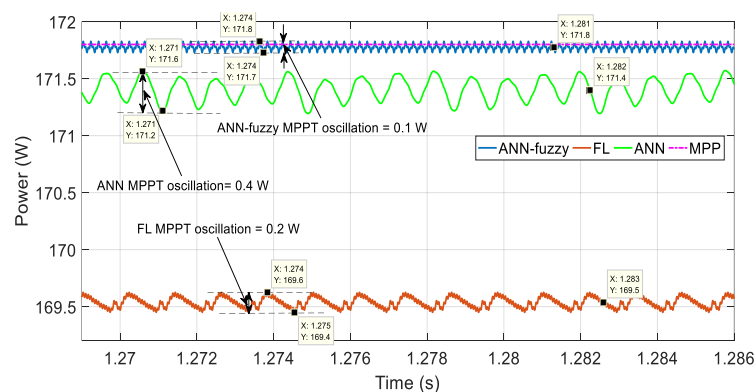


Figure 25. FL, ANN, and ANN-fuzzy MPPT power ripple MPPT techniques during the change of insolation from 500 W/m^2 to 800 W/m^2

Figures 26 and 27 demonstrate how the intended MPPT controllers track MPP with respect to the weather profile indicated in the previous figure. The graph shows MPP tracking utilizing developed MPPT controllers that have been tested using the aforementioned weather profile. The irradiance is reduced from

800 W/m² to 600 W/m² for the final period $t \in [1, 5, 2]$ s at $T = 25$ °C. The ANN-fuzzy and ANN controllers closely followed the MPP, and in both cases, the power levels were extremely near to the predicted values corresponding to the irradiation and temperature rates specified in this instance. The power value supplied by using the FL controller is less accurate than those for ANN-fuzzy and ANN controllers. Furthermore, the ANN-fuzzy methodology significantly excels the other two approaches in terms of tracking accuracy. The proposed ANN-fuzzy MPPT regulator responds to variations in sunlight and achieves the steady-state operating point in 2 ms, as can be observed in Figure 26. The FL controller enters a steady state regime after 13 ms of decreasing irradiation, whereas the ANN MPPT controller needs 14 ms. In comparison to the other methods, the FLMPPT controller delivers a less precise power value. Additionally, the reaction times for the FL MPPT and ANN MPPT approaches are 6.5 and 7 times slower than those for the ANN-fuzzy MPPT controller. All methods have the advantage of not overshooting during the transient phase, which allows them to avoid energy losses during the transient regime. From Figure 27, the proposed algorithm ANN-fuzzy behaves well in a steady state regime under the specified climatic factors of this case, and this strategy produces a smooth power curve, almost without steady state oscillation. The ripple around MPP created by the ANN method at steady state is 0.2 W, which is 0.155% of the power value obtained by this methodology, resulting in significant energy loss for a PV system. The FL algorithm provides a less precise power value than the other two approaches, with a steady-state ripple of 0.1 W (0.079%). As a result, the system's dynamic response and steady-state performance are good when using the proposed ANN-fuzzy technique. In addition, the recommended ANN-fuzzy method has good tracking speed compared to the other simulated algorithms.

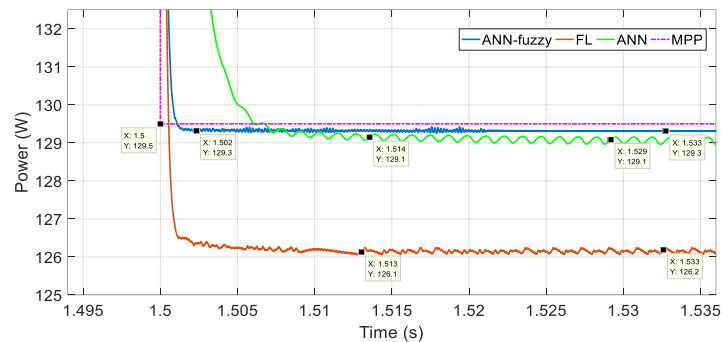


Figure 26. Response time of the FL, ANN, and ANN-fuzzy during the change of insolation from 800 W/m² to 600 W/m²

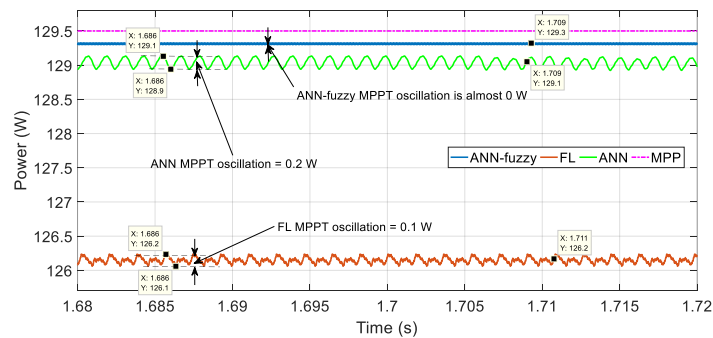


Figure 27. FL, ANN, and ANN-fuzzy MPPT power ripple MPPT techniques during the change of insolation from 800 W/m² to 600 W/m²

4.1.1. Efficiency during irradiation variation

Efficiency is a crucial factor to consider when evaluating any MPPT technique. Furthermore, to assess the precision of the power results, the MPPT efficiency is calculated using the following [6], [16].

$$\eta_{MPPT} = \frac{P_{measured}}{P_{theoretical}} \times 100 \quad (6)$$

P_{measured} denotes the computed power using the FL MPPT, ANN MPPT, or ANN-fuzzy MPPT. $P_{\text{theoretical}}$ is the estimated theoretical MPP value that the PV panel will deliver for a given temperature and irradiance. To compare the ANN-fuzzy MPPT, the FL MPPT, and the ANN MPPT in terms of mean tracking efficiency, these performances are compiled in Table 4. According to the results displayed in Table 4, the ANN-fuzzy MPPT exhibits great efficiency and outperforms both the ANN MPPT and FL MPPT for any abrupt change in irradiance.

Table 4. Efficacy evaluation of the FL, ANN, and ANN-fuzzy methodologies under varying irradiance

Irradiation (W/m ²)	MPP (W)	MPPT (FL technique) (W)	MPPT (ANN technique) (W)	MPPT (ANN- fuzzy technique) (W)	Efficiency FL MPPT (%)	Efficiency ANN MPPT (%)	Efficiency ANN-fuzzy MPPT (%)
500	108	104.3	107.3	107.8	96.57	99.35	99.81
600	129.5	126.2	129.1	129.3	97.45	99.69	99.84
800	171.8	169.5	171.4	171.8	98.66	99.76	100
1,000	213.1	212.4	212.2	212.7	99.67	99.57	99.81
Average					98.08	99.59	99.86

4.2. Results under variation of temperature

Figure 28 depicts the temperature profile, with an irradiation of 1,000 W/m² during the simulation (2 seconds), and the initial temperature is set at $T=25^{\circ}\text{C}$ from zero to 0.5 s. Following that, abrupt temperature changes occur at 0.5 s, 1 s, and 1.5 s. The corresponding temperature ranges are 25 to 35, 35 to 45, and 45 to 20 °C. The different MPPT systems described in this research paper will be evaluated using their accuracy, tracking efficiency, convergence speed, overshoot in the transient phase, and oscillation around the peak power point. Figure 29 shows the responses of various MPPT control strategies under varying temperature conditions.

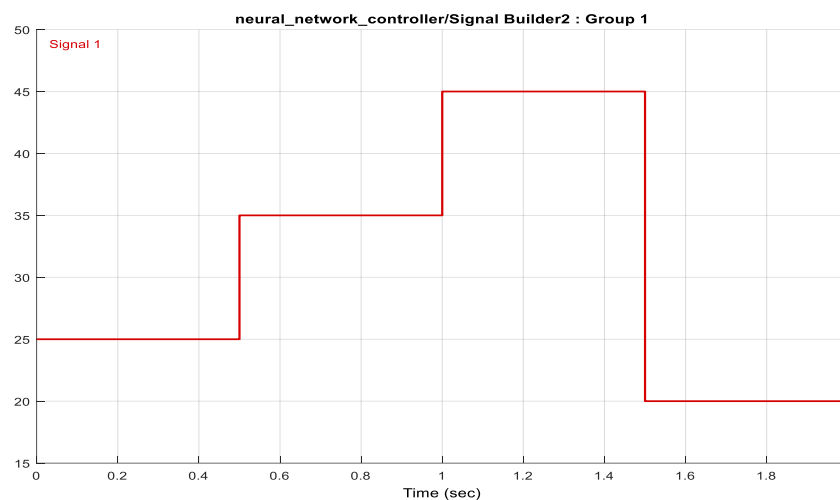


Figure 28. Simulation temperature rate

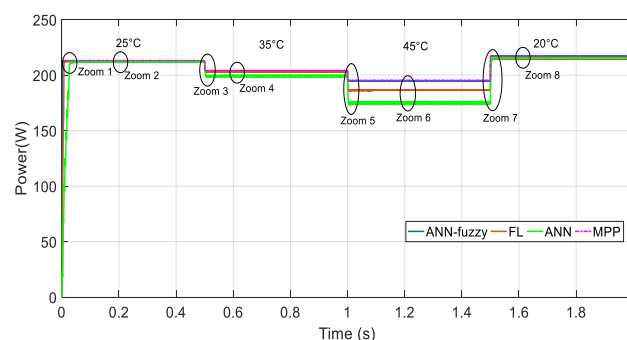


Figure 29. The output power of the PV system under scenario II of temperature variation as simulated using the FL, ANN, and the proposed ANN-fuzzy MPPT techniques

The outcomes in the first interval when $t \in [0, 0.5]$ are identical to those in the previous situation. (See Figures 20 and 21 in the previous section, "results under variation of irradiation"). Figures 30 and 31 show MPP monitoring utilizing MPPT controllers that were designed and simulated using the abovementioned environmental factors. When the temperature is 35°C and the radiation is $1,000\text{ W/m}^2$, for the second period $t \in [0.5, 1]$ s, the MPP is tracked correctly by the ANN-fuzzy MPPT controller, and in this case, the power value is very close to the expected MPP for the specified temperature and irradiation. Although the FL controller's power value is less accurate than that produced by the ANN-fuzzy controller, it is still acceptable. The ANN MPPT controller is the least accurate in terms of tracking the MPP among all the algorithms presented earlier in these irradiation and temperature conditions. Furthermore, compared to the other two methods, the ANN-fuzzy approach allows for more precise tracking of the highest power point MPP produced by the PV panel. The suggested ANN-fuzzy MPPT controller responds to temperature changes and reaches the steady state operating point in 0.6 ms when the temperature is increased from 25°C to 35°C and for solar irradiation $G=1,000\text{ W/m}^2$, as shown in Figure 30. We also observe an overshoot of 0.3 W (0.147%) when using the ANN-fuzzy MPPT technique, but this last quickly restarts the peak point tracking operation. The FL MPPT controller responds to the temperature change in 2 ms , while the ANN MPPT controller needs 7.4 ms . The ANN MPPT controller produces an inaccurate power value compared to the other approaches. We can also see that the FL MPPT and ANN MPPT techniques have response times that are 3.33 times and 12.33 times slower than the ANN-fuzzy MPPT controller, respectively. According to Figure 31, the proposed algorithm ANN-fuzzy and FL techniques behave well in a steady state under the specific climate circumstances for this case, with a low steady state oscillation of 0.1 W for the ANN-fuzzy method. This value represents 0.049% of the power value achieved by this technique, and 0.2 W for the FL method, which represents 0.0985% of the power value reached when using this technique. The power value supplied by the ANN algorithm is less accurate than the other two methods, with a significant ripple of 1.4 W (0.7%) at steady state. This causes an important energy loss for the PV system.

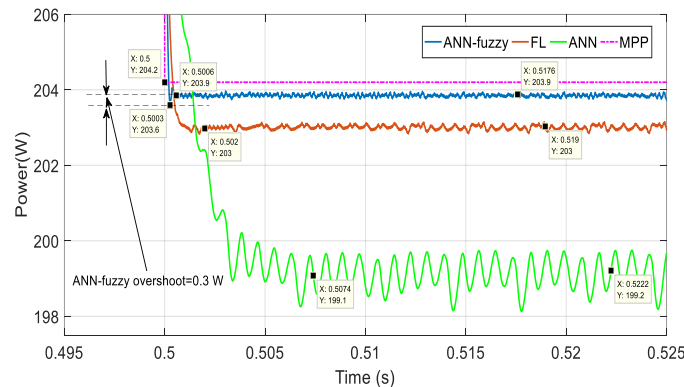


Figure 30. Response time of the FL, ANN, and ANN-fuzzy MPPT during the change of temperature from 25°C to 35°C

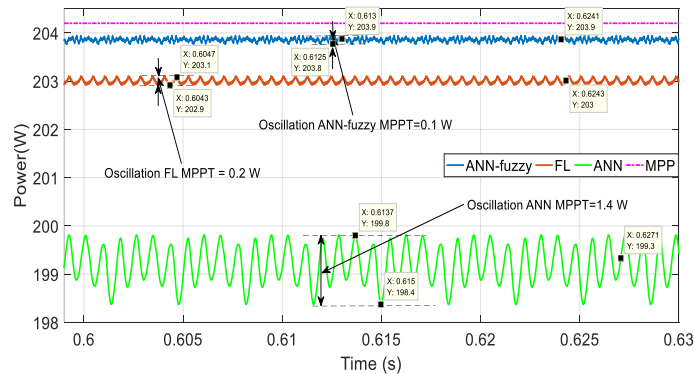


Figure 31. The FL, ANN, and ANN-fuzzy MPPT power ripple techniques during the change of temperature from 25°C to 35°C

Figures 32-34 illustrate MPP tracking via constructed and simulated MPPT controllers based on the weather profile shown above. For the third interval $t \in [1, 1.5]$ s, the insulation is $G = 1,000 \text{ W/m}^2$, and the temperature is $T = 45^\circ\text{C}$. The ANN-fuzzy MPPT controller accurately tracked the MPP, as evidenced by the power value provided by this last, which is extremely close to the theoretical value matched to the sunshine and temperature conditions specified in this instance. The FL and ANN MPPT controllers fail to follow the theoretical MPP value, especially for the power value produced by the ANN controller, which is far from the MPP in this case. The tracking accuracy of the peak power point generated by the PV array is, in this case, significantly better with the ANN-fuzzy algorithm than with other methods.

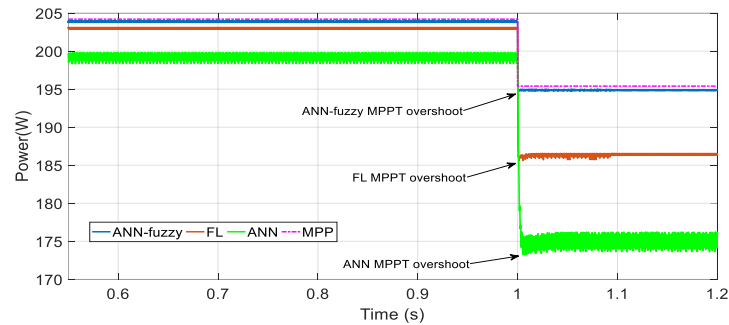


Figure 32. Overshoot of the FL, ANN, and the proposed ANN-fuzzy MPPT techniques during the change of temperature from 35°C to 45°C

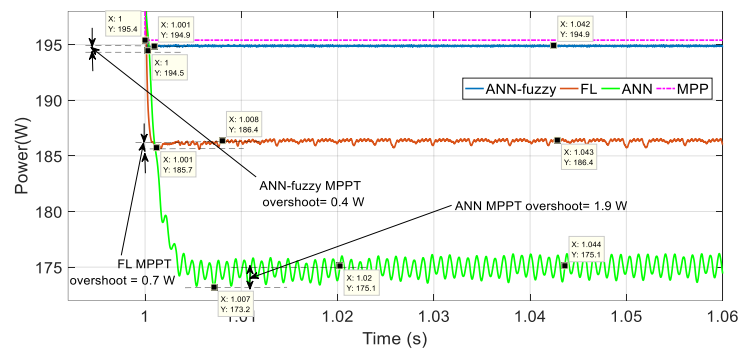


Figure 33. Response time of the FL, ANN, and ANN-fuzzy MPPT techniques during the change of temperature from 35°C to 45°C

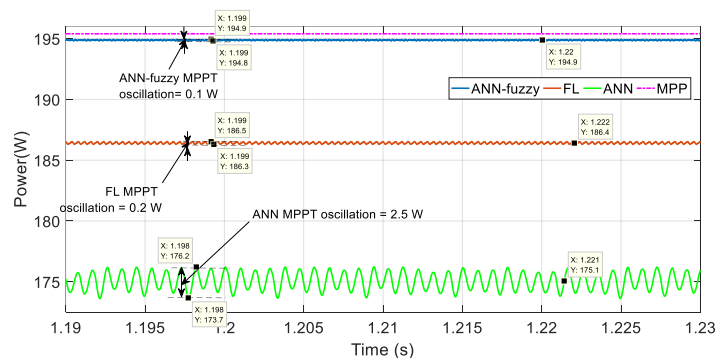


Figure 34. FL, ANN, and ANN-fuzzy MPPT power ripple during the change of temperature from 35°C to 45°C

When the temperature increases from 35°C to 45°C and the irradiation is $1,000 \text{ W/m}^2$, the proposed ANN-fuzzy MPPT controller responds to temperature variations and achieves the steady state operating point in 1 ms. The FL controller reaches steady state after 8 ms, while the ANN MPPT controller takes 20 ms. Both the ANN and FL MPPT controllers give a less precise power value than the ANN-fuzzy approach. We can also see that the ANN MPPT and FL MPPT techniques have response times that are 20 times and 8 times

slower than the ANN-fuzzy MPPT controller, respectively. We also observe an overshoot of 0.4 W (0.2%) when using the ANN-fuzzy MPPT technique. However, it rapidly restarts the maximum point tracking operation. The FL and ANN MPPT approaches induced significant overshoot that was more than that produced by the ANN-fuzzy technique, which results in increased energy loss during the transient period. The FL MPPT overshoot is 0.7 W (0.375%), while the ANN MPPT overshoot is 1.9 W (1.085%). From Figure 34, the suggested algorithm ANN-fuzzy performs well in a steady state under the particular weather conditions in this instance, with a low steady state oscillation of 0.1 W for the ANN-fuzzy method. This value represents 0.051% of the power value produced by this technique. Regarding the FL MPPT method, the ripple around MPP caused by this technique at steady state is 0.2 W, which represents 0.107% of the power value reached by this technique. The power value supplied by the ANN algorithm is less accurate than the other two methods, with a large amount of oscillation of 2.5 W (1.427%) at steady state; this results in significant energy waste for a PV system.

Figures 35 and 36 show how the designed MPPT controllers respond to tracking the MPP against the weather profile presented in the previous section. During the last interval, the temperature is $T=20\text{ }^{\circ}\text{C}$ and the insolation is $G=1,000\text{ W/m}^2$, $t \in [1.5, 2]$ s. The ANN-fuzzy controller closely followed the MPP, as shown by the power value delivered by the PV system using this last control unit. This is quite near to the predicted values associated with the specific solar irradiation and temperature in this situation. Compared to the ANN-fuzzy MPPT controller, the ANN MPPT controller generates a less accurate power value. However, it is a reasonable value. The power value provided by the FL controller is less accurate than the ANN-fuzzy and ANN controller values. In terms of tracking accuracy, the ANN-fuzzy methodology performs noticeably better than the other two methods. As shown in Figure 35, the proposed ANN-fuzzy MPPT controller responds to temperature changes and reaches the steady-state operating point when the temperature drops from $45\text{ }^{\circ}\text{C}$ to $20\text{ }^{\circ}\text{C}$ and the illumination is maintained constant at $1,000\text{ W/m}^2$ in 1 ms.

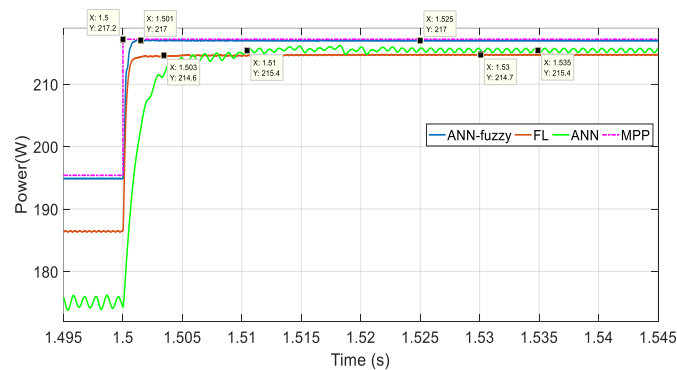


Figure 35. Response time of the FL, ANN, and ANN-fuzzy MPPT during the change of temperature from $45\text{ }^{\circ}\text{C}$ to $20\text{ }^{\circ}\text{C}$

The FL controller enters a steady state after 3 ms of decreasing the temperature, whereas the ANN MPPT controller needs 10 ms. Compared to the other methods, the FLMPPT controller provides a less accurate power value. We can also see that the response times of the FL MPPT and ANN MPPT methods are respectively 3 times and 10 times slower than those of the ANN-fuzzy MPPT controller. All methods have the advantage of not overshooting (undershooting) during the transient phase, which allows them to avoid energy losses during the transient regime. In Figure 36, the suggested algorithms ANN-fuzzy perform well in a steady state under the specified meteorological conditions. In this case, the power curve produced by this methodology is nearly smooth, with a small steady-state oscillation of 0.1 W (0.046%). For the ANN method, the fluctuations caused by this technique at steady state are more important than the oscillations caused by the two other methods 0.6 W, which represents 0.279% of the power value attained by this technique. For a PV system, this led to considerable energy waste. Compared to the other two approaches, the FL algorithm's power value is less precise, with a steady state ripple of 0.2 W (0.093%). When using the ANN-fuzzy approach, the system's dynamic responsiveness and steady-state performance are therefore good. The ANN-fuzzy method that was suggested has a faster tracking speed than the other simulated approaches.

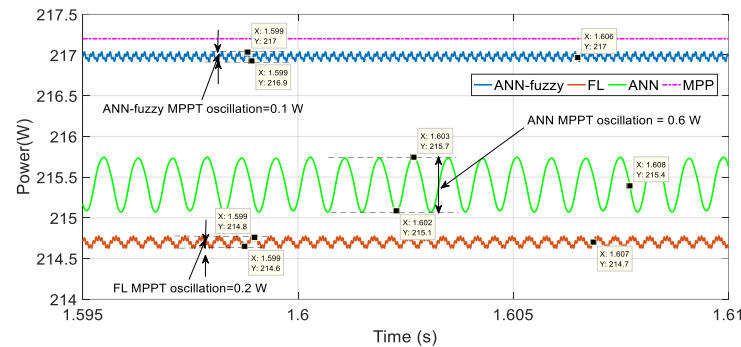


Figure 36. The FL, ANN, and ANN-fuzzy MPPT power ripple techniques during the change of temperature from 45 °C to 20 °C

4.2.1. Efficiency during temperature variation

Table 5 depicts the efficiency of our system under various temperature conditions. The findings indicate that for any sudden change in temperature, the ANN-fuzzy MPPT performs better than both the ANN MPPT and the FL MPPT. In this case, its average efficiency is 99.825%

Table 5. Efficacy comparison of the FL, ANN, and ANN-fuzzy methodologies when the temperature varies

Temperature (°C)	MPP (W)	MPPT (FL technique) (W)	MPPT (ANN technique) (W)	MPPT (ANN-fuzzy technique) (W)	Efficiency FL MPPT (%)	Efficiency ANN MPPT (%)	Efficiency ANN-fuzzy MPPT (%)
25	213.1	212.4	212.2	212.7	99.67	99.57	99.81
35	204.2	203	199.2	203.9	99.41	97.55	99.85
45	195.4	186.4	175.1	194.9	95.39	89.61	99.74
20	217.2	214.7	215.4	217	98.85	99.17	99.9
Average					98.33	96.475	99.825

5. CONCLUSION

In this work, we examined how solar systems monitor their highest power points. The MPPT controllers discussed in this paper were developed using FL, ANN, and the suggested ANN-fuzzy approach (combining the two methods previously mentioned). After that, they are tested in the MATLAB/Simulink environment using a simulated PV system in various test conditions. The suggested controllers are then evaluated using a comparative study that takes into account factors including accuracy, efficiency, convergence speed, transient overshoot, and steady-state oscillation around the MPP. The simulation outcomes demonstrate the effectiveness of the suggested ANN-fuzzy MPPT controller in both transient and steady state regimes, as proven by the fact that the proposed strategy outperforms both FL and ANN MPPT controllers in terms of tracking the MPPs quickly and precisely under standard test conditions and a variety of suddenly changing meteorological conditions (irradiation and temperature). The major contribution of this research paper is the combining of the two approaches previously described and the exploitation of each method's benefits, such as the ANN technique's learning capacity and the FL method's quick tracking and precision. On the other hand, reducing the number of rules utilized by the FL component of the hybrid ANN-fuzzy MPPT controller to 7 instead of 25 in the majority of publications in the literature allows the cost of this control unit to be optimized.

REFERENCES




- [1] H. G. Ali, R. V. Arbos, J. Herrera, A. Tobón, and J. P-Restrepo, "Non-Linear Sliding Mode Controller for Photovoltaic Panels with Maximum Power Point Tracking," *Processes*, vol. 8, no. 1, p. 108, Jan. 2020, doi: 10.3390/pr8010108.
- [2] G. Masson and I. Kaizuka, "Strategic PV Analysis and Outreach," *International Energy Agency Photovoltaic Power Systems Programme*, 2022. [Online]. Available: https://iea-pvps.org/research-tasks/strategic-pv-analysis-outreach/contacts_t1/. (Access 24th October 2022).
- [3] "2022: The Year of Terawatt Solar Global installed solar capacity expected to hit Terawatt mark in early 2022," *Solar Power Europe*, Jan. 2022. [Online]. Available: <https://www.solarpowereurope.org/news/2022-the-year-of-terawatt-solar/>. (Access 24th October 2022).
- [4] M. Kermadi and E. M. Berkouk, "Artificial intelligence-based maximum power point tracking controllers for Photovoltaic systems: Comparative study," *Renewable and Sustainable Energy Reviews*, vol. 69, pp. 369–386, Mar. 2017, doi: 10.1016/j.rser.2016.11.125.

- [5] "Solar 1000 MW: les lers kilowattheures photovoltaïques produits vers la fin 2023-Economie," *El Moudjahid*. [Online]. Available: <https://www.elmoudjahid.dz/fr/economie/solar-1000-mw-les-lers-kilowattheures-photovoltaïques-produits-vers-la-fin-2023-185488> (Access 24th October 2022).
- [6] M. Ahmed, I. Harbi, R. Kennel, M. L. Heldwein, J. Rodríguez, and M. Abdelrahem, "Performance Evaluation of PV Model-Based Maximum Power Point Tracking Techniques," *Electronics*, vol. 11, no. 16, p. 2563, Aug. 2022, doi: 10.3390/electronics11162563.
- [7] E. J. Yun, J. T. Park, and C. G. Yu, "An maximum power point tracking interface circuit for low-voltage DC-type energy harvesting sources," *Bulletin of Electrical Engineering and Informatics*, vol. 11, no. 6, pp. 3108–3118, Dec. 2022, doi: 10.11591/eei.v11i6.4124.
- [8] J. H. Kumar, S. B. Ch, and J. Yugandhar, "Design and Investigation of Short Circuit Current Based Maximum Power Point Tracking for Photovoltaic System," *Science Academy Publisher International Journal of Research and Reviews in Electrical and Computer Engineering*, vol. 1, no. 2, pp. 2046–5149, Jul. 2011.
- [9] K. Ullah, Y. Wang, A. Zaman, H. Imtiaz, S. Ahmad, and B. Kumar, "Maximum Power Point Technique (MPPT) for PV System Based on Improved Pert and Observe (P&O) Method with PI Controller," *International Research Journal of Engineering and Technology (IRJET)*, vol. 6, no. 12, pp. 813–819, Dec. 2019.
- [10] L. Merabet, A. Ourici, and T. Wafa, "Efficiency of perturb and observe mppt for pv system with boost converter," *BEST: International Journal of Management Information Technology and Engineering (BEST: IJMITE)*, vol. 8, p. 14, Nov. 2021.
- [11] S. Salman, X. AI, and Z. WU, "Design of a P&O algorithm based MPPT charge controller for a stand-alone 200 W PV system," *Protection and Control of Modern Power Systems*, vol. 3, no. 1, Aug. 2018, doi: 10.1186/s41601-018-0099-8.
- [12] S. Motahhir, A. E. Hammoumi, and A. E. Ghzizal, "Photovoltaic system with quantitative comparative between an improved MPPT and existing INC and P&O methods under fast varying of solar irradiation," *Energy Reports*, vol. 4, pp. 341–350, Nov. 2018, doi: 10.1016/j.egyr.2018.04.003.
- [13] A. A. AlZubaidi, L. A. Khaliq, H. S. Hamad, W. K. Al-Azzawi, M. S. Jabbar, and T. A. Shihab, "MPPT implementation and simulation using developed P&O algorithm for photovoltaic system concerning efficiency," *Bulletin of Electrical Engineering and Informatics*, vol. 11, no. 5, pp. 2460–2470, Oct. 2022, doi: 10.11591/eei.v11i5.3949.
- [14] D. Choudhary and A. Saxena, "Incremental Conductance MPPT Algorithm for PV System Implemented Using DC-DC Buck and Boost Converter," *International Journal of Engineering Research and Applications*, vol. 4, no. 8, pp. 123–132, Aug. 2014.
- [15] L. Shang, H. Guo, and W. Zhu, "An improved MPPT control strategy based on incremental conductance algorithm," *Protection and Control of Modern Power Systems*, vol. 5, no. 1, Jun. 2020, doi: 10.1186/s41601-020-00161-z.
- [16] S. Necaibia, M. S. Kelaiaia, H. Labar, A. Necaibia, and E. D. Castronuovo, "Enhanced auto-scaling incremental conductance MPPT method, implemented on low-cost microcontroller and SEPIC converter," *Solar Energy*, vol. 180, pp. 152–168, Mar. 2019, doi: 10.1016/j.solener.2019.01.028.
- [17] R. Kerid and Y. Bounnah, "Modeling and parameter estimation of solar photovoltaic based MPPT control using EKF to maximize efficiency," *Bulletin of Electrical Engineering and Informatics*, vol. 11, no. 5, pp. 2491–2499, Oct. 2022, doi: 10.11591/eei.v11i5.3782.
- [18] C. R. Algarín, J. T. Giraldo and O. R. Álvarez, "Fuzzy Logic Based MPPT Controller for a PV System," *Energies*, vol. 10, no. 12, p. 2036, Dec. 2017, doi: 10.3390/en10122036.
- [19] T. Zhu, J. Dong, X. Li, and S. Ding, "A Comprehensive Study on Maximum Power Point Tracking Techniques Based on Fuzzy Logic Control for Solar Photovoltaic Systems," *Frontiers in Energy Research*, vol. 9, Jul. 2021, doi: 10.3389/fenrg.2021.727949.
- [20] R. M. Asif *et al.*, "Design and analysis of robust fuzzy logic maximum power point tracking based isolated photovoltaic energy system," *Engineering Reports*, vol. 2, no. 9, Jul. 2020, doi: 10.1002/eng2.12234.
- [21] S. Messalti, A. Harrag, and A. Loukriz, "A new variable step size neural networks MPPT controller: Review, simulation and hardware implementation," *Renewable and Sustainable Energy Reviews*, vol. 68, pp. 221–233, Feb. 2017, doi: 10.1016/j.rser.2016.09.131.
- [22] A. F. Toure, F. Danioko, and B. Diourte, "Application of Artificial Neural Networks for Maximal Power Point Tracking," *International Journal of Sustainable and Green Energy*, vol. 10, no. 2, p. 40, 2021, doi: 10.11648/j.ijrse.20211002.12.
- [23] M. H. Parvaneh and P. G. Khorasani, "A new hybrid method based on Fuzzy Logic for maximum power point tracking of Photovoltaic Systems," *Energy Reports*, vol. 6, pp. 1619–1632, Nov. 2020, doi: 10.1016/j.egyr.2020.06.010.
- [24] A. Kumar, A. Kumar, and R. Arora, "Overview of Genetic Algorithm Technique for maximum Power Point Tracking (MPPT) of Solar PV System," *IJCA Proceedings on Innovations in Computing and Information Technology (Cognition 2015)*, vol. COGNITION 2015, no. 3, pp. 21–24, Jul. 2015.
- [25] T. A. Wani *et al.*, "A Review of Fuzzy Logic and Artificial Neural Network Technologies Used for MPPT," *Turkish Journal of Computer and Mathematics Education (TURCOMAT)*, vol. 12, no. 2, pp. 2912–2918, Apr. 2021, doi: 10.17762/turcomat.v12i2.2327.
- [26] A. R. Reisi, M. H. Moradi, and S. Jamsab, "Classification and comparison of maximum power point tracking techniques for photovoltaic system: A review," *Renewable and Sustainable Energy Reviews*, vol. 19, pp. 433–443, Mar. 2013, doi: 10.1016/j.rser.2012.11.052.
- [27] B. Subudhi and R. Pradhan, "A Comparative Study on Maximum Power Point Tracking Techniques for Photovoltaic Power Systems," *IEEE Transactions on Sustainable Energy*, vol. 4, no. 1, pp. 89–98, Jan. 2013, doi: 10.1109/tste.2012.2202294.
- [28] Z. Salam, J. Ahmed, and B. S. Merugu, "The application of soft computing methods for MPPT of PV system: A technological and status review," *Applied Energy*, vol. 107, pp. 135–148, Jul. 2013, doi: 10.1016/j.apenergy.2013.02.008.
- [29] P. Bhatnagar and R. K. Nema, "Maximum power point tracking control techniques: State-of-the-art in photovoltaic applications," *Renewable and Sustainable Energy Reviews*, vol. 23, pp. 224–241, Jul. 2013, doi: 10.1016/j.rser.2013.02.011.
- [30] A. Mellit and S. A. Kalogirou, "MPPT-based artificial intelligence techniques for photovoltaic systems and its implementation into field programmable gate array chips: Review of current status and future perspectives," *Energy*, vol. 70, pp. 1–21, Jun. 2014, doi: 10.1016/j.energy.2014.03.102.
- [31] H. Rezk, M. Aly, M. Al-Dhaifallah, and M. Shoyama, "Design and Hardware Implementation of New Adaptive Fuzzy Logic-Based MPPT Control Method for Photovoltaic Applications," *IEEE Access*, vol. 7, pp. 106427–106438, 2019, doi: 10.1109/access.2019.2932694.
- [32] C. Napole, M. Derbeli, and O. Barambones, "Fuzzy Logic Approach for Maximum Power Point Tracking Implemented in a Real Time Photovoltaic System," *Applied Sciences*, vol. 11, no. 13, p. 5927, Jun. 2021, doi: 10.3390/app11135927.
- [33] M. A. Danandeh and S. M. M. G, "A new architecture of INC-fuzzy hybrid method for tracking maximum power point in PV cells," *Solar Energy*, vol. 171, pp. 692–703, Sep. 2018, doi: 10.1016/j.solener.2018.06.098.




- [34] D. Remoaldo and I. Jesus, "Analysis of a Traditional and a Fuzzy Logic Enhanced Perturb and Observe Algorithm for the MPPT of a Photovoltaic System," *Algorithms*, vol. 14, no. 1, p. 24, Jan. 2021, doi: 10.3390/a14010024.
- [35] H. Rezk and A. M. Eltamaly, "A comprehensive comparison of different MPPT techniques for photovoltaic systems," *Solar Energy*, vol. 112, pp. 1–11, Feb. 2015, doi: 10.1016/j.solener.2014.11.010.
- [36] L. Hichem, M. Leila, and O. Amar, "Comparative Study of Perturb-and-Observe and Fuzzy Logic MPPT for Stand-Alone PV System," in *Artificial Intelligence and Heuristics for Smart Energy Efficiency in Smart Cities*, Springer International Publishing, 2021, pp. 266–276, doi: 10.1007/978-3-030-92038-8_27.
- [37] M. Fathi and J. A. Parian, "Intelligent MPPT for photovoltaic panels using a novel fuzzy logic and artificial neural networks based on evolutionary algorithms," *Energy Reports*, vol. 7, pp. 1338–1348, Nov. 2021, doi: 10.1016/j.egyr.2021.02.051.
- [38] D. S. R. K. Mukesh Kumar, "Comparison between IC and Fuzzy Logic MPPT Algorithm Based Solar PV System using Boost Converter," *International Journal of Advanced Research in Electrical, Electronics and Instrumentation Engineering*, vol. 04, no. 06, pp. 4927–4939, Jun. 2015, doi: 10.15662/ijareeie.2015.0406007.
- [39] T. Ramalu, M. M. Radzi, M. M. Zainuri, N. A. Wahab, and R. A. Rahman, "A Photovoltaic-Based SEPIC Converter with Dual-Fuzzy Maximum Power Point Tracking for Optimal Buck and Boost Operations," *Energies*, vol. 9, no. 8, p. 604, Jul. 2016, doi: 10.3390/en9080604.
- [40] U. Yilmaz, A. Kircay, and S. Borekci, "PV system fuzzy logic MPPT method and PI control as a charge controller," *Renewable and Sustainable Energy Reviews*, vol. 81, pp. 994–1001, Jan. 2018, doi: 10.1016/j.rser.2017.08.048.
- [41] W. Na, P. Chen, and J. Kim, "An Improvement of a Fuzzy Logic-Controlled Maximum Power Point Tracking Algorithm for Photovoltaic Applications," *Applied Sciences*, vol. 7, no. 4, p. 326, Mar. 2017, doi: 10.3390/app7040326.
- [42] U. H. Salman, S. F. Nawaf, and M. O. Salih, "Studying and analyzing the performance of photovoltaic system by using fuzzy logic controller," *Bulletin of Electrical Engineering and Informatics*, vol. 11, no. 3, pp. 1687–1695, Jun. 2022, doi: 10.11591/eei.v11i3.3680.
- [43] R. Sharmin, S. S. Chowdhury, F. Abedin, and K. M. Rahman, "Implementation of an MPPT technique of a solar module with supervised machine learning," *Frontiers in Energy Research*, vol. 10, Aug. 2022, doi: 10.3389/fenrg.2022.932653.
- [44] F. Sedaghati, A. Nahavandi, M. A. Badamchizadeh, S. Ghaemi, and M. A. Fallah, "PV Maximum Power-Point Tracking by Using Artificial Neural Network," *Mathematical Problems in Engineering*, vol. 2012, pp. 1–10, 2012, doi: 10.1155/2012/506709.
- [45] V. K. Viswambaran, D. A. Bati, and D. E. Zhou, "Review of AI Based Maximum Power Point Tracking Techniques & Performance Evaluation of Artificial Neural Network based MPPT Controller for Photovoltaic Systems," *International Journal of Advanced Science and Technology*, vol. 29, no. 10s, pp. 8159–8171, Jun. 2020.

BIOGRAPHIES OF AUTHORS






Louki Hichem    received a Bachelor of Science in engineering in 2015 from the Preparatory School for Science and Technology in Annaba, Algeria, and a Master of Science with an Engineering Degree in Electrical Engineering from the National Polytechnic School of Constantine, Algeria, in 2018. Currently, he is pursuing a Ph.D. in electrical engineering from the Department of Electrical Engineering at BADJI Mokhtar-Annaba University in Algeria. His research interests include renewable energy system modeling and control. He can be contacted at email: hichem.louki@univ-annaba.org.



Omeiri Amar    was born in Skikda, Algeria, in 1958. He received the Engineer degree from Annaba University in 1983, Master degree of Science by research from Strathclyde University, UK in 1986 and the Ph.D. degree in 2007 from Annaba University, Algeria. Since 1987 He has been a Lecturer at Annaba University in the Electrical Engineering department. His current research field includes active power filters, renewable energies, power electronics, AC, and DC drives. He can be contacted at email: omeiri.amar@gmail.com.



Merabet Leila    received Engineer (electrical engineering) and Magister (electrical control) degrees from Annaba University in 1993 and 2001 respectively. She had her Ph.D degree in 2015 and the "Habilitation to supervise research" degree on electrical engineering in 2019. She is working as senior researcher "A". Her research interest includes renewable energy systems, power quality, harmonics, control, PV system, and artificial neuron networks. She authored and co-authored many papers in academic journals, conferences and proceedings. She can be contacted at email: lei_elt@yahoo.fr.